BAROTROPIC PREDICTION OF 500-MB AND 100-MB FLOW PATTERNS

by

HAROLD M. WOOLF

S.B., Massachusetts Institute of Technology

(1960)

SUBMITTED IN PARTIAL FULFILLMENT OF THE

REQUIREMENTS FOR THE DEGREE OF

MASTER OF SCIENCE

at the

MASSACHUSETTS INSTITUTE OF TECHNOLOGY

June, 1961

Signature of Author...
Department of Meteorology, May 20, 1961

Certified by.... ....
Thesis Supervisor

Accepted by...
Chairman, Departmental Committee on
Graduate Students

BAROTROPIC PREDICTION OF 500-MB AND 100-MB FLOW PATTERNS

by

Harold M. Woolf

Submitted to the Department of Meteorology on May 20, 1961, in partial fulfillment of the requirements for the degree of Master of Science.

ABSTRACT

Vertical profiles of mean zonal wind component at 30, 40, and 50 degrees North Latitude imply that the equivalent-barotropic levels defined by Charney and Eliassen (1949) are located between the 500-mb and 400-mb levels, and very near the 100-mb level. An investigation was carried out in order to ascertain whether or not 100-mb flow behaves, and can be predicted, barotropically. The equivalent-barotropic prognostic equation was integrated numerically on the IBM 709 computer. Forecasts were made for periods of 24 and 48 hours during an active situation, for 500 mb as well as 100 mb to provide a basis for comparison of results.

The results of the numerical prediction indicate that while the 100-mb forecast errors are small, a lower degree of forecast skill is displayed at that level than at 500 mb. In every forecast period the barotropic technique predicted excessive eastward displacement of the 100-mb trough. A field of large-scale divergence, which would be neglected in the equivalent-barotropic procedure, was postulated as the source of this systematic error. Supplementary computations were performed, and a plausible hypothetical divergence pattern was deduced therefrom.

The value of the 100-mb prognostic charts in wind forecasting was also investigated. Geostrophic winds determined from these charts yielded root-mean-square vector errors substantially smaller than the errors in persistence forecasts, for periods of both 24 and 48 hours. However, in view of the small data-sample obtained, it was concluded only tentatively that the method presented is a generally useful and valuable 100-mb wind-prediction technique.

With respect to both the barotropic-prediction and wind-forecasting phases of the investigation, it was concluded that considerable additional study is both necessary and desirable.

This thesis was done in part at the MIT Computation Center, Cambridge, Massachusetts.

Thesis Supervisor: Frederick Sanders

Title: Associate Professor of Meteorology

ACKNOWLEDGMENT

To Prof. Frederick Sanders of the MIT Meteorology Department, who as thesis advisor provided many helpful suggestions and much encouragement during the course of this project, the author wishes to express his sincere appreciation.

The author is grateful to Mr. Sidney Teweles of the United States Weather Bureau for providing the 100-mb analyses used in this thesis.

The services of Miss Leola Odland, Meteorology Department programmer, and of the staff and facilities of the MIT Computation Center are also appreciated.

The assistance of Mr. A. James Wagner in analyzing several of the charts presented in this report is gratefully acknowledged.

Special thanks are due to Miss Isabel Kole for preparing the many figures for publication.

TABLE OF CONTENTS

FIGURES AND TABLES

SYMBOLS

x	east-west horizontal coordinate
y	north-south horizontal coordinate
p	pressure, vertical coordinate
t	time
Z	geopotential height of a constant-pressure surface
$\mathbb{V}$	horizontal wind velocity vector
$\mathbb{V}_{nd}$	non-divergent part of horizontal wind
ζ	vertical component of relative vorticity
f	coriolis parameter, $2\Omega \sin\phi$, where Ω = angular velocity of the earth, ϕ = latitude
f_o	"standard," constant value of f, equal to $10^{-4}\sec^{-1}$
ω	vertical "velocity," $\frac{dp}{dt}$
$A(p)$	equivalent-barotropic modeling coefficient
$(\ )_G$	value of ( ) at the surface of the earth
u	mean zonal wind

I. INTRODUCTION

The equivalent-barotropic model, proposed by Charney and Eliassen (1949), was the first numerical weather prediction scheme to be tested by means of high-speed digital computers, and according to Ellsaesser (1960) has been in operational use by the Joint Numerical Weather Prediction Unit since 1956. It has been applied, in research as well as in routine forecasting, principally to flow at the 500-mb level. Certain theoretical considerations, which are related in the following section of this report, led the author to believe that significant results might be obtained by barotropic prediction of flow at 100 mb. As a by-product of the purely scientific interest of the problem, namely the investigation of the computational consequences of a theoretical proposition, an engineering application was realized--the use of a 100-mb prognostic chart, once obtained, as an aid to wind forecasting. The prediction of winds at the 100-mb level, at an altitude of approximately 16 km, is certainly a practical problem, for military aviation at present and for commercial operations in the not-too-distant future. While the major effort in this study has been devoted to the portion of the problem of greatest scientific interest, consideration has been given to the engineering aspect as well.

II. THEORETICAL DISCUSSION

A. Equivalent-Barotropic Vorticity Equation

Phillips (1958) has presented a clear and concise development of the prediction equation for Charney and Eliassen's (1949) model. The starting point is the vorticity equation in (x,y,p,t) coordinates, exact except for the assumption of hydrostatic equilibrium and the neglect of friction:

$$\frac{\partial \zeta}{\partial t} + \mathbb{V} \cdot \nabla (f+\zeta) + \omega \frac{\partial \zeta}{\partial p} + (f+\zeta) \nabla \cdot \mathbb{V} + \frac{\partial \omega}{\partial x}\frac{\partial v}{\partial p} - \frac{\partial \omega}{\partial y}\frac{\partial u}{\partial p} = 0, \quad (1)$$

If the geostrophic approximation is made, Charney's (1948) scale considerations permit one to simplify Eq. (1) to a great extent by neglecting terms that are one or more orders of magnitude smaller than the principal terms of the equation. By also making use of the (x,y,p,t) form of the equation of continuity

$$\nabla \cdot \mathbb{V} + \frac{\partial \omega}{\partial p} = 0, \quad (2)$$

one may then write the simpler vorticity equation

$$\frac{\partial \zeta}{\partial t} + \mathbb{V} \cdot \nabla (f+\zeta) - f_0 \frac{\partial \omega}{\partial p} = 0. \quad (3)$$

The fundamental modeling approximation is twofold: firstly, the direction of the non-divergent part of the wind is invariant with, or independent of, height or pressure above a given point; secondly, the same vertical profile of non-divergent-wind speed is valid at all points (x,y,t). The simple mathematical expression of this relationship is

$$\mathbb{V}_{nd}(x,y,p,t) = A(p)\,\overline{\mathbb{V}}_{nd}(x,y,t) \tag{4}$$

where $\overline{(\ )} \equiv \frac{1}{p_G}\int_0^{p_G}(\ )dp$, the average with respect to pressure of the quantity ( ). It is obvious from Eq. (4) that $\overline{A} = 1$.

Substitution of Eq. (4) into Eq. (3) gives

$$A\left[\frac{\partial\overline{\zeta}}{\partial t} + \overline{\mathbb{V}}_{nd}\cdot\nabla f\right] + A^2\,\overline{\mathbb{V}}_{nd}\cdot\nabla\overline{\zeta} - f_0\frac{\partial\omega}{\partial p} = 0. \tag{5}$$

Pressure-averaging or "barring" of Eq. (5) yields

$$\frac{\partial\overline{\zeta}}{\partial t} + \overline{\mathbb{V}}_{nd}\cdot\nabla f + \overline{A^2}\,\overline{\mathbb{V}}_{nd}\cdot\nabla\overline{\zeta} - \frac{f_0\,\omega_G}{p_G} = 0. \tag{5a}$$

Let $\mathbb{V}^* = \overline{A^2}\,\overline{\mathbb{V}}_{nd}$, hence $\zeta^* = \overline{A^2}\,\overline{\zeta}$. Then Eq. (5a) can be written

$$\frac{\partial\zeta^*}{\partial t} + \mathbb{V}^*\cdot\nabla(f+\zeta^*) - \frac{\overline{A^2}\,f_0\,\omega_G}{p_G} = 0. \tag{6}$$

Except over strongly sloping terrain, the last term in Eq. (6) can be neglected, leaving the equivalent-barotropic vorticity equation in its simplest form:

$$\frac{\partial \zeta^*}{\partial t} + \mathbb{V}^* \cdot \nabla (f + \zeta^*) = 0, \tag{7}$$

which states that the absolute vorticity is conserved following the horizontal motion at the "star" level(s), where $A = \overline{A^2}$. This is the form of the equation employed in the present investigation.

B. <u>Determination of Equivalent-Barotropic Levels</u>

The equivalent-barotropic or "star" levels in the atmosphere can be determined from actual wind data, or if the geostrophic approximation is made, from isobaric height data. Buch's (1954) northern hemisphere mean winter wind data indicate that at 30, 40, and 50 degrees North Latitude, $A = \overline{A^2}$ between 500 mb and 400 mb, and slightly above 100 mb (see Table A.2). This fact led the author to initiate this study, in order to determine whether or not flow at the 100-mb level behaves barotropically.

For the case studied in this project, the equivalent-barotropic levels were determined geostrophically for 30, 40, and 50 degrees North Latitude, between 70 and 125 degrees

West Longitude (see Table A.1), at the initial time of the forecast period, 1200 GCT 18 November 1957. The results show the levels to be almost exactly at 100 mb, and near 400 mb. The two levels for which forecasts were made are 100 mb and 500 mb; the effect of making a barotropic forecast for a non-barotropic level is discussed in a later section of this thesis (see Section IV., Part B.).

III. PREPARATION OF PROGNOSTIC CHARTS

A. The Initial Synoptic Situation

The most prominent feature of the situation, and the one of greatest interest for the subsidiary wind-forecasting study, is the deep trough (hemispheric wave number six) located over central North America (see Figs. 1, 3, 7). While there are other features of interest on the initial maps (Fig. 1), forecasts of their future behavior were expected to be quite poor, principally because of the boundary constraints. Further comment on this point may be found in Section IV., Part B.

The situation was studied for a 48-hour period, from 1200 GCT 18 November 1957 to 1200 GCT 20 November.

B. The Computational Procedure

The prognostic calculations were performed on the IBM 709 Electronic Data Processing Machine of the MIT Computation Center. The program had been previously prepared by members of the Dynamical Forecasting Project of the MIT Meteorology Department. Input information consists of isobaric height values in decafeet on a rectangular grid of 486 points (27 x 18), with diagonal grid-point separation of five degrees of latitude, or 300 nautical miles.

The simple equivalent-barotropic vorticity equation (Eq. (7)) is transformed into the finite-difference analog of a Poisson equation, which is then solved by relaxation for the local rate of change of isobaric height, $\partial Z/\partial t$. Iterative integration in time ($\Delta t = 45$ minutes) yields predicted height values which then become the initial data for a new Poisson equation. The relaxation-iteration procedure continues until the end of the desired period, whereupon the forecast height values in decafeet are printed out by the computer. The values were transcribed to a grid overprinted on the standard MIT Meteorology Department North American Base Map, and analyzed in the usual fashion.

Forecasts were made for both levels under study for periods of 24 and 48 hours with 1200 GCT 18 November as the initial time, and for 24 hours with 1200 GCT 19 November as the initial time.

The computer program also yielded grid-point values of absolute vorticity at each print-out stage, which though not displayed in Section IV., Part A., proved to be of value for supplementary calculations presented and discussed in Part B. of Section IV.

IV. RESULTS OF BAROTROPIC PREDICTION

A. Presentation

In the figures on the following twelve pages are presented charts of initial, forecast, and observed isobaric height patterns, observed height change, and forecast error (predicted minus observed) patterns for all of the initial and verification times and forecast periods of the case. The upper portion of each figure, designated (a), refers to conditions at the 500-mb level; the lower portion, designated (b), to 100 mb. All contours are labeled in tens of feet; on the isobaric height maps, the tens of thousands digits are omitted, following conventional meteorological practice. The omitted digits are one for 500 mb and five for 100 mb.

B. Discussion

Some qualitative assessments of the probable "goodness" of the various forecasts were made before the actual prognostic computations were performed. Solution of the finite-difference Poisson equation by relaxation on a rectangular grid requires arbitrary specification of boundary values; it has been general practice in problems of this nature, followed in the computer program used in the preparation of the material presented here, to fix the initial boundary height values for all time. It was therefore expected that

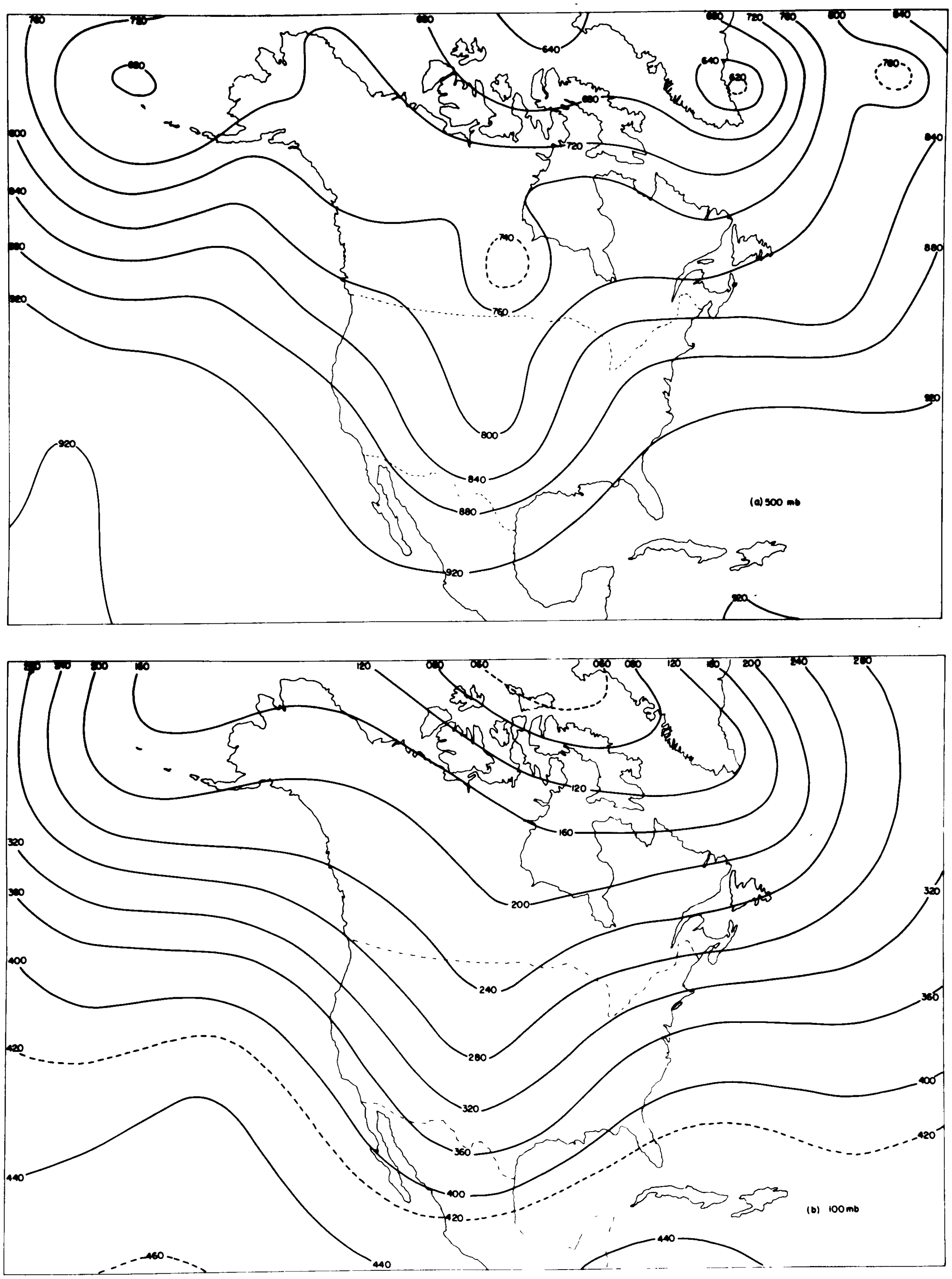

Figure 1. Observed heights, 1200 GCT 18 November 1957.

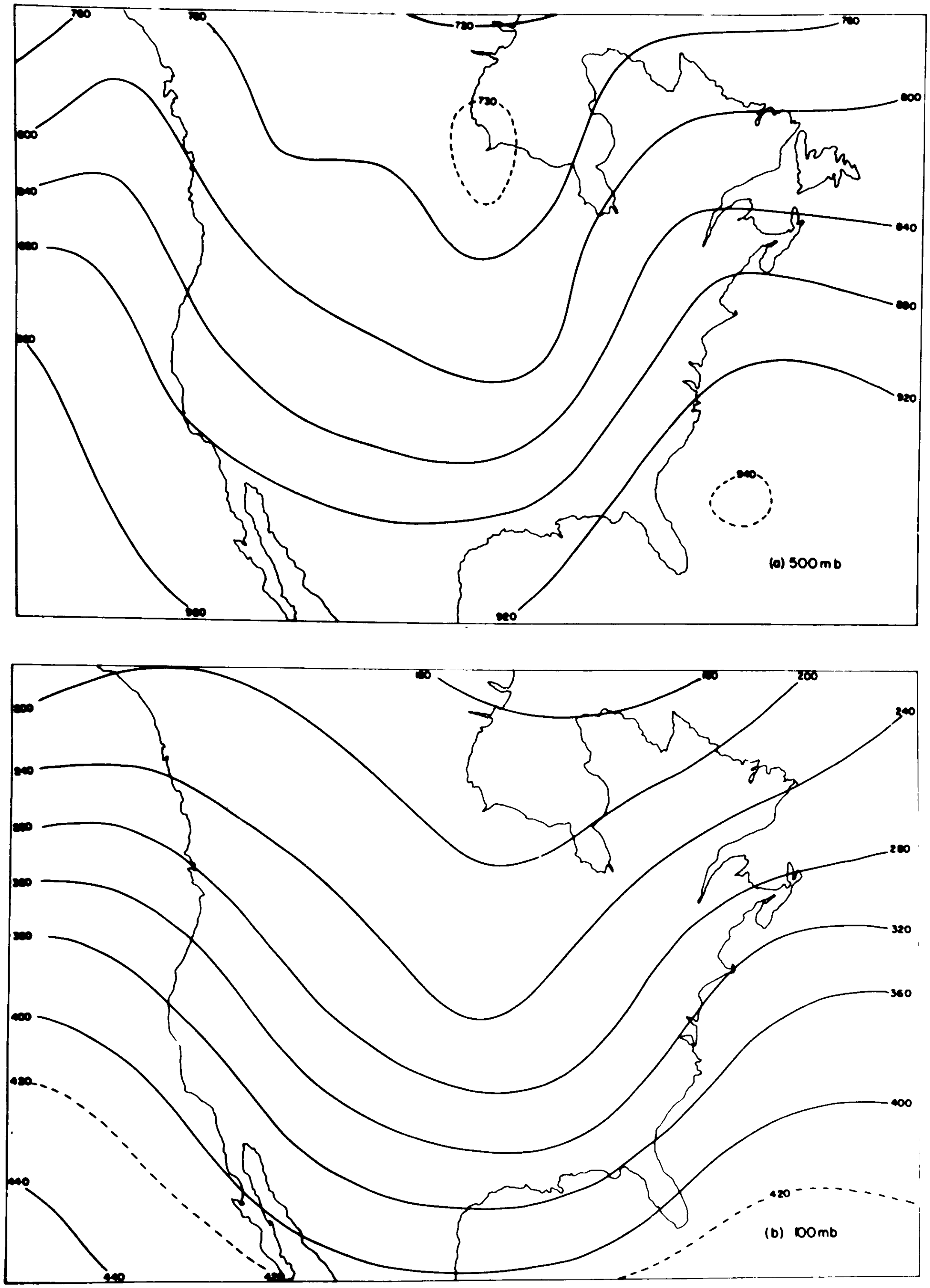

Figure 2. 24-hour barotropic forecasts for 1200 GCT 19 November 1957.

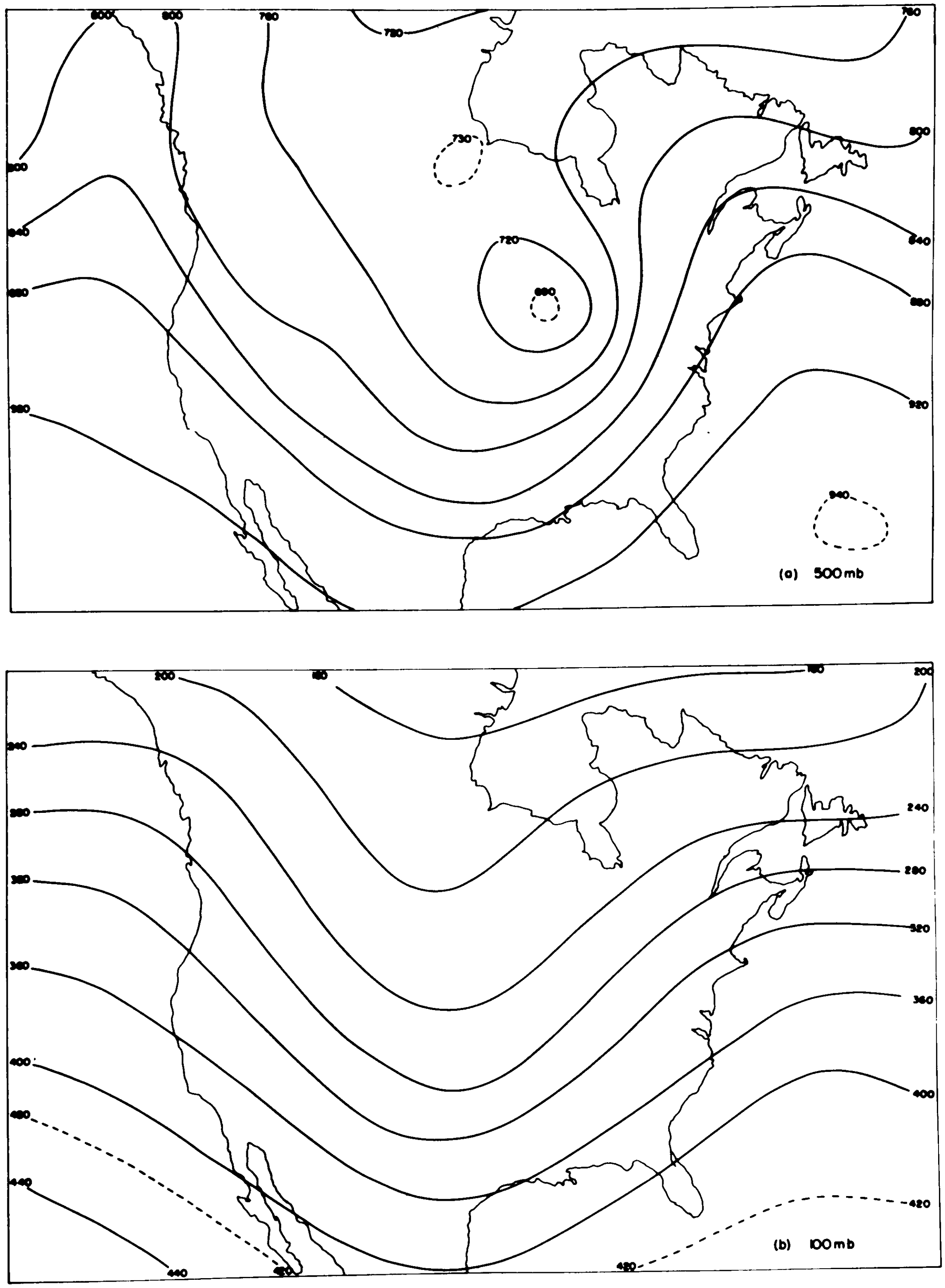

Figure 3. Observed heights, 1200 GCT 19 November 1957.

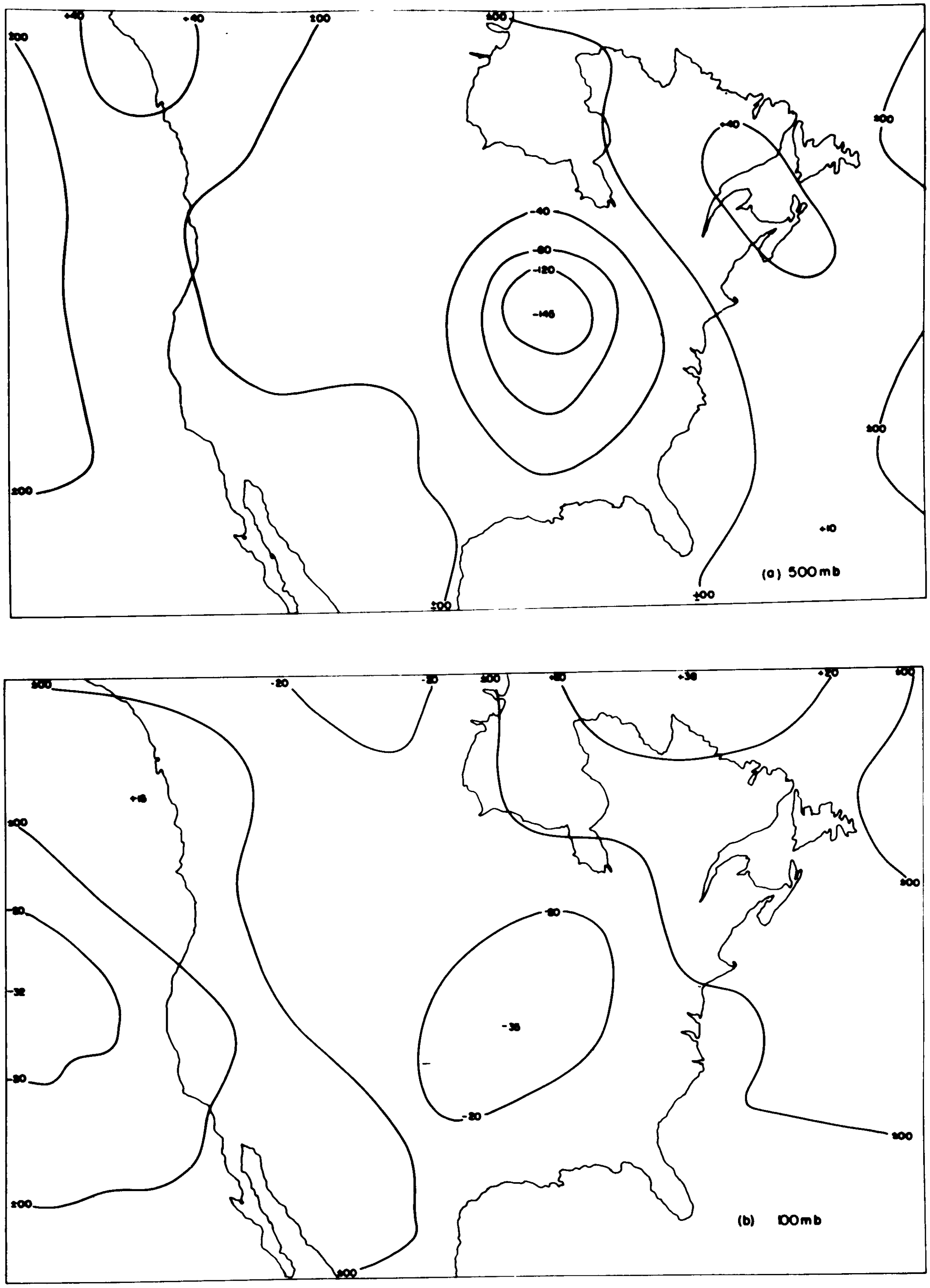

<u>Figure 4</u>. Observed 24-hour height changes, from 1200 GCT 18 November to 1200 GCT 19 November.

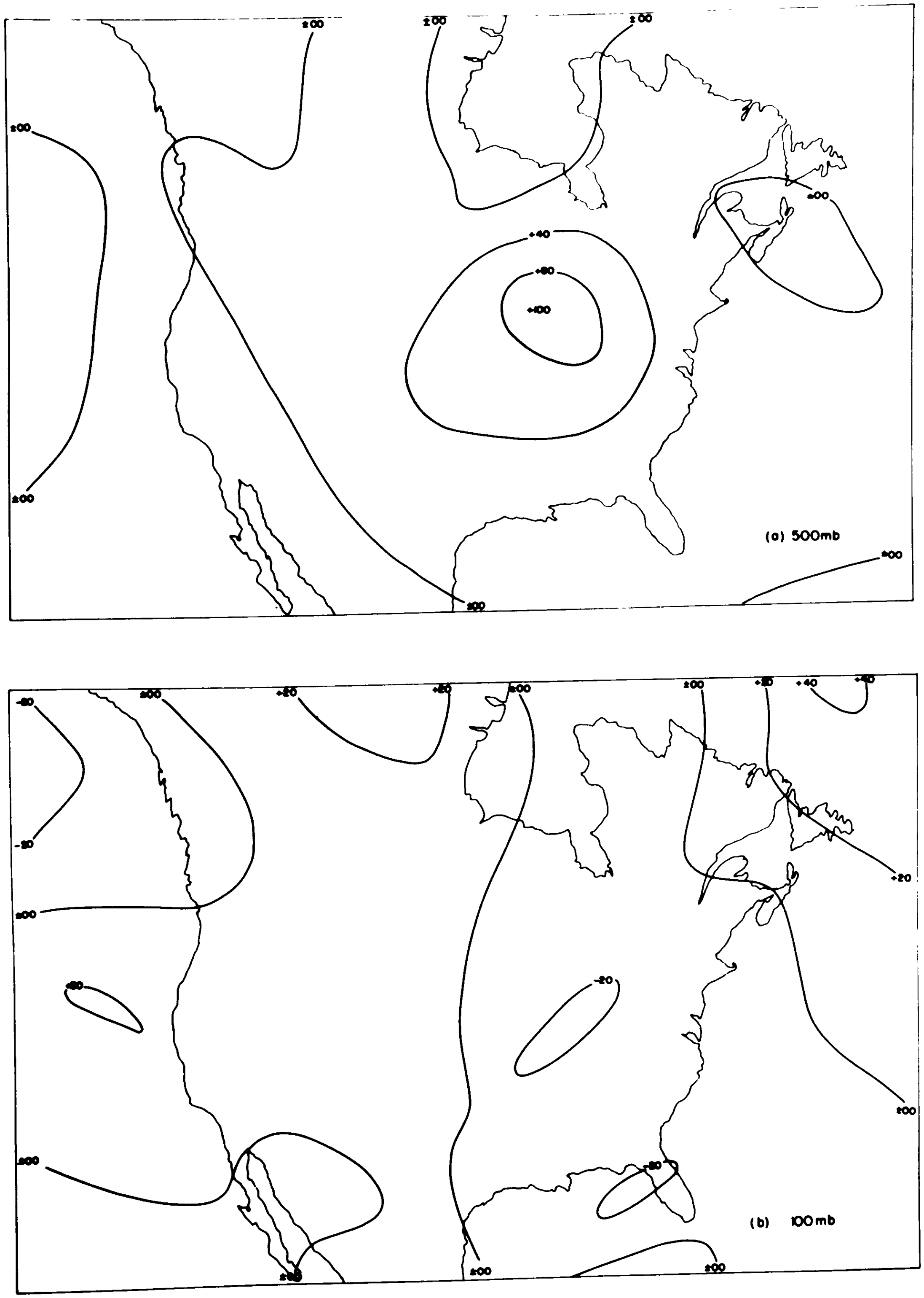

<u>Figure 5</u>. 24-hour-forecast errors, 1200 GCT 19 November.

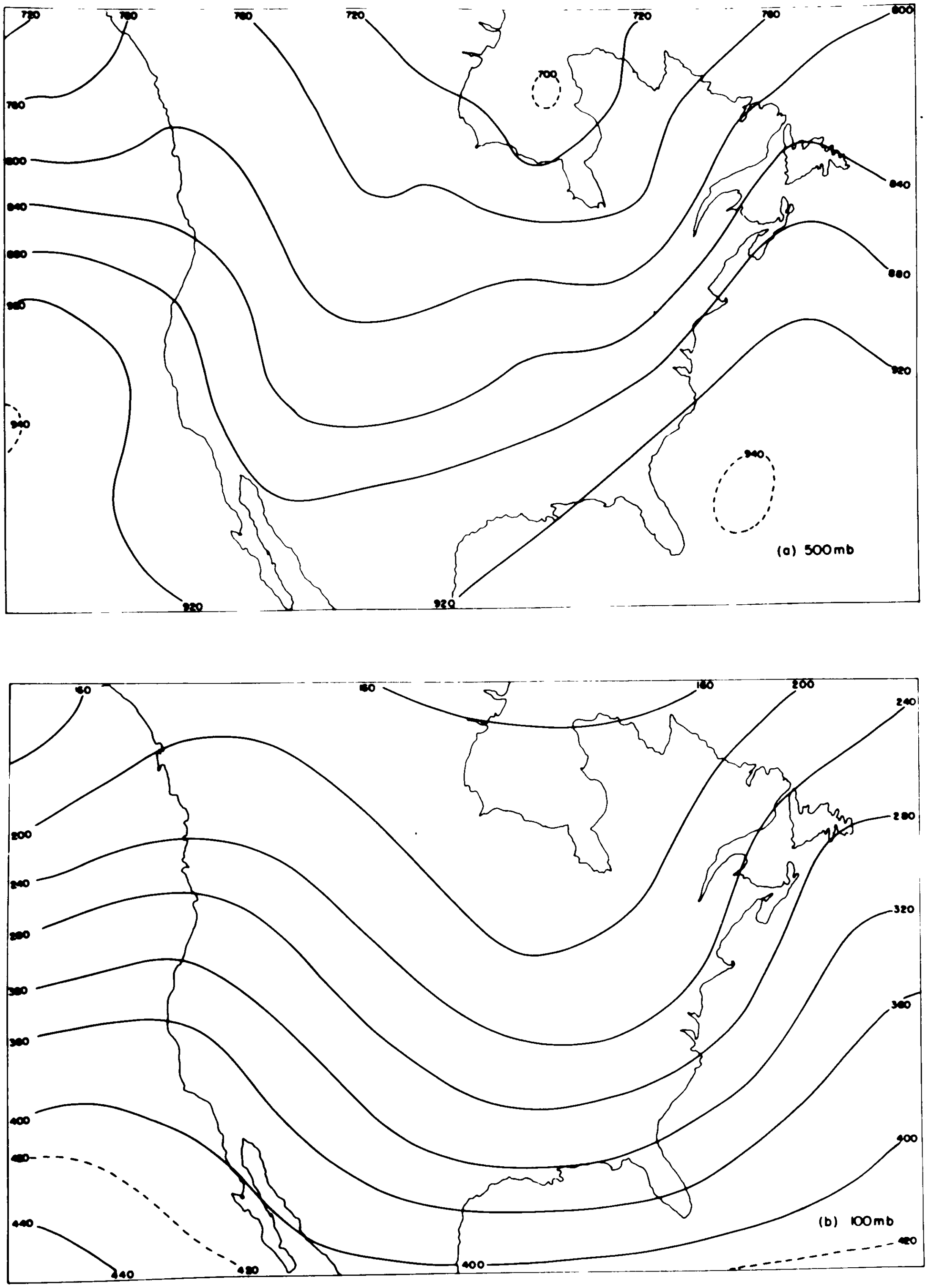

Figure 6. 48-hour barotropic forecasts for 1200 GCT 20 November.

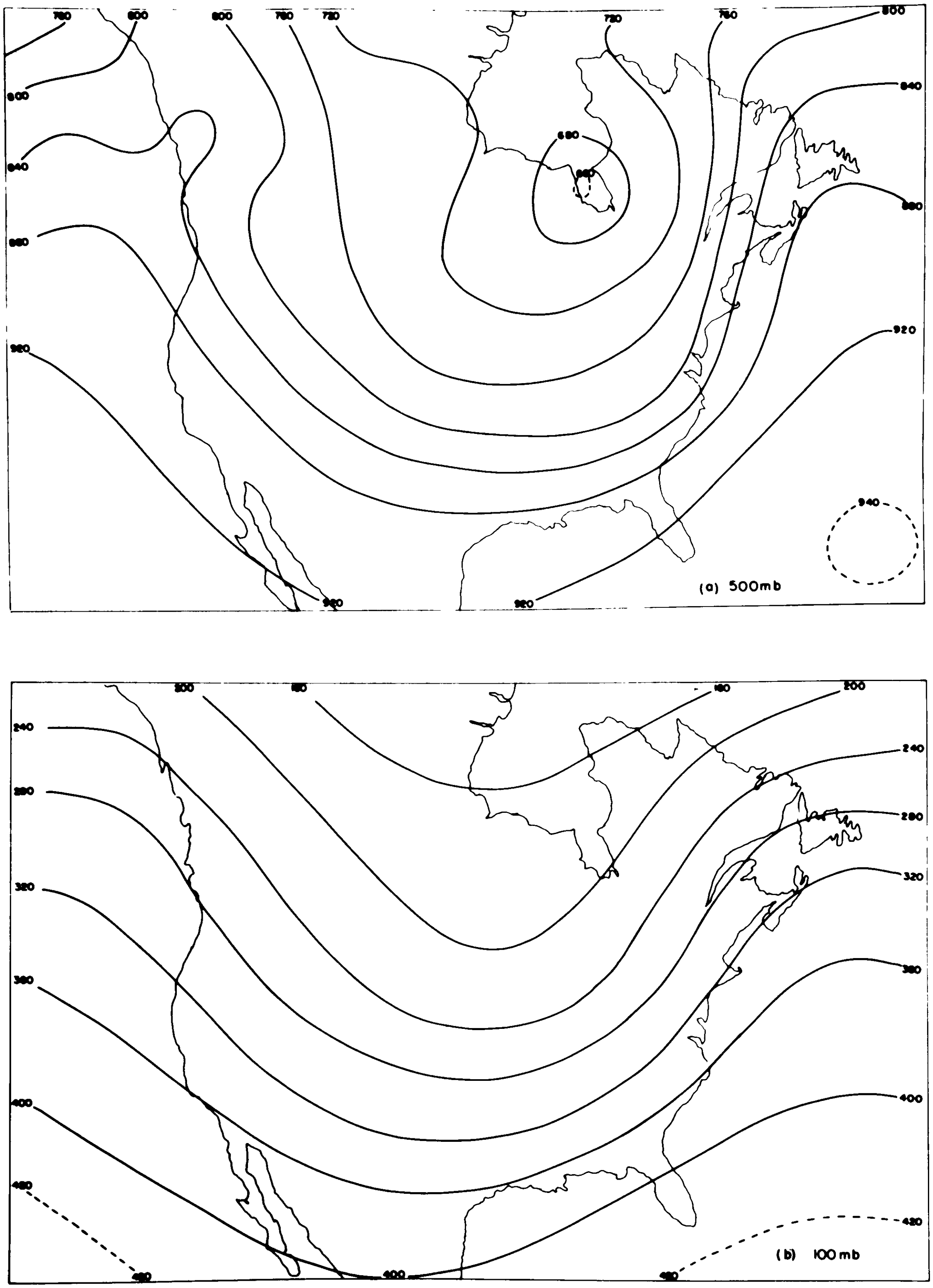

Figure 7. Observed heights, 1200 GCT 20 November.

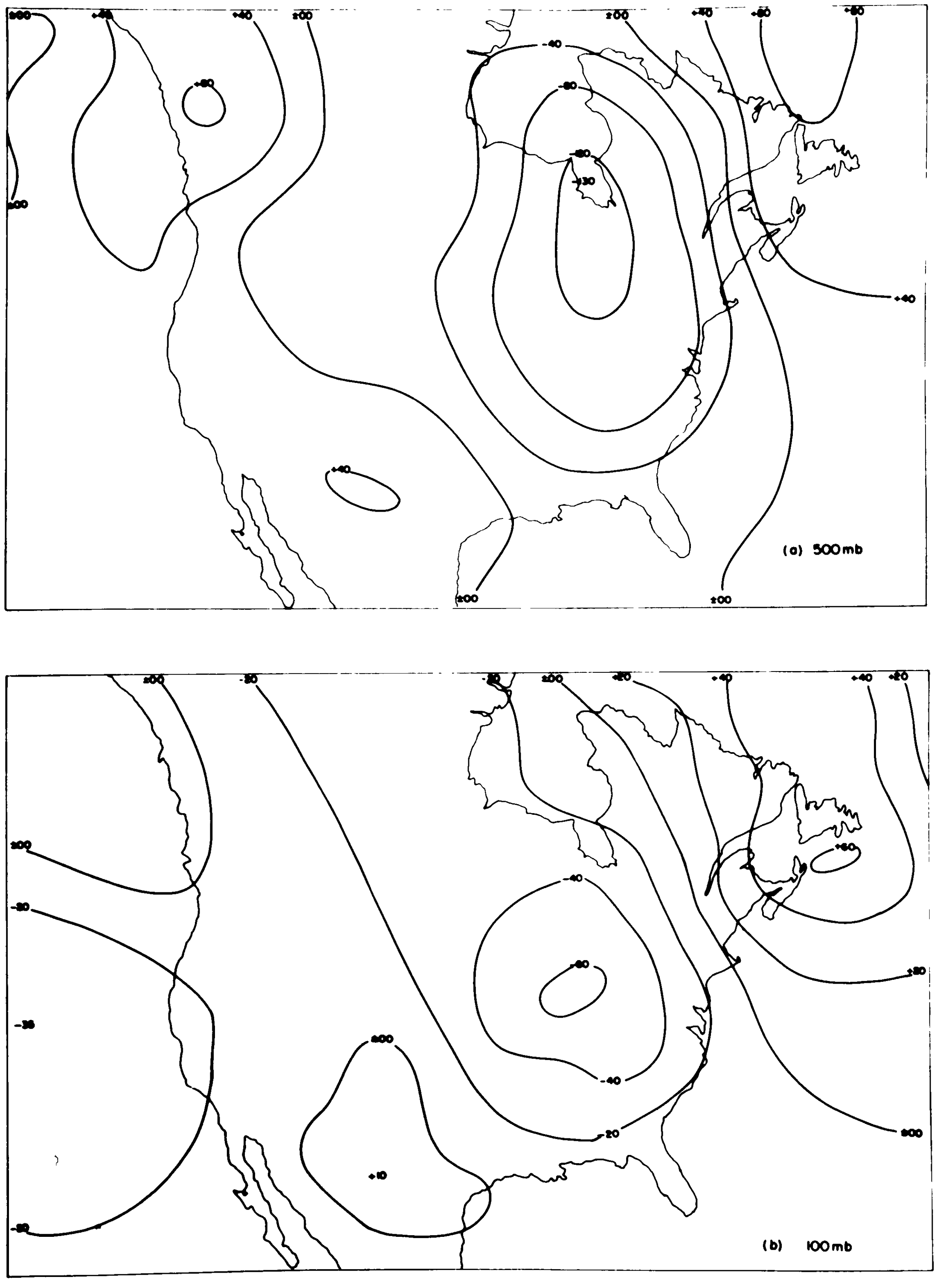

<u>Figure 8</u>. Observed 48-hour height changes, from 1200 GCT 18 November to 1200 GCT 20 November.

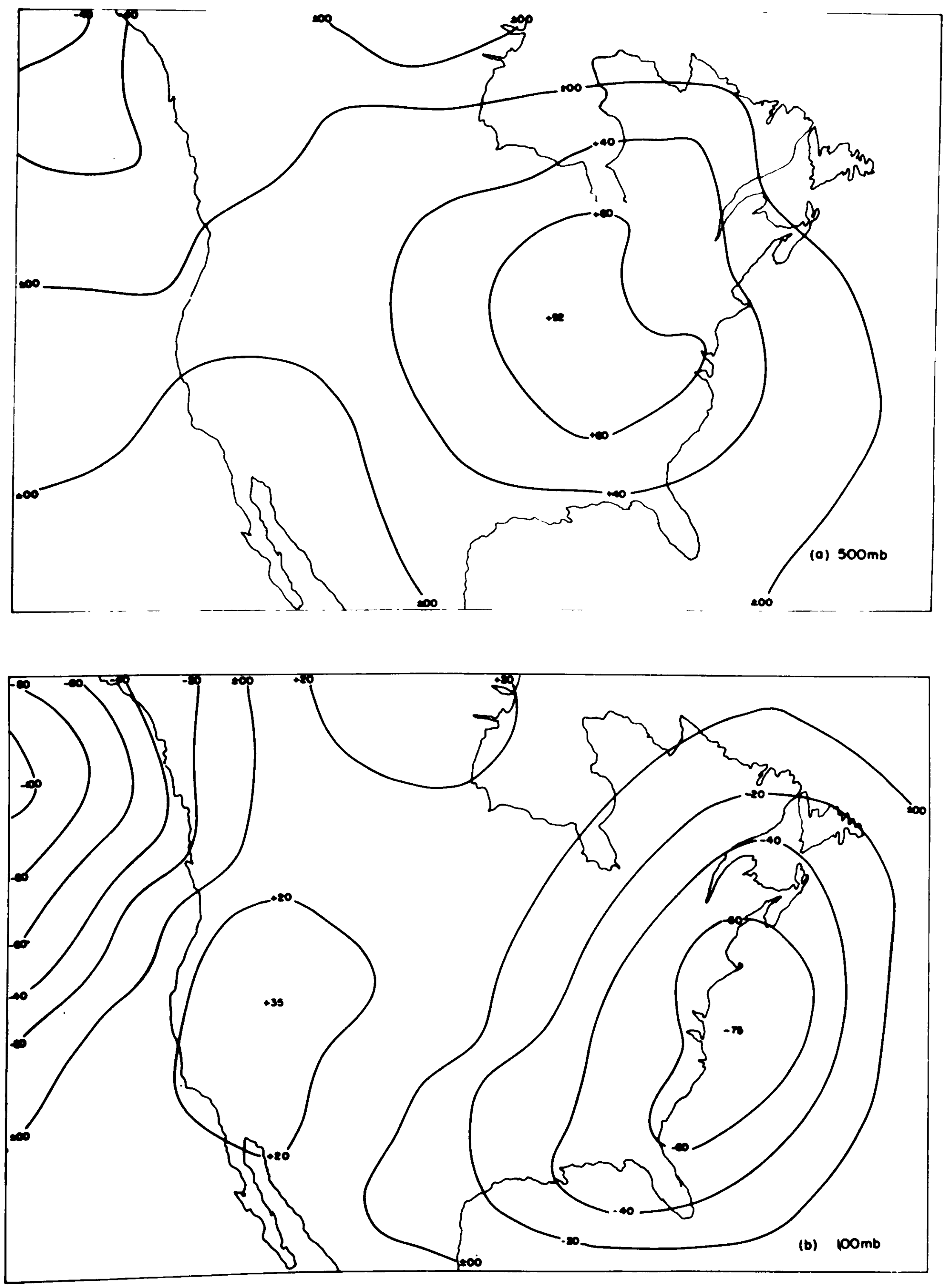

Figure 9. 48-hour-forecast errors, 1200 GCT 20 November.

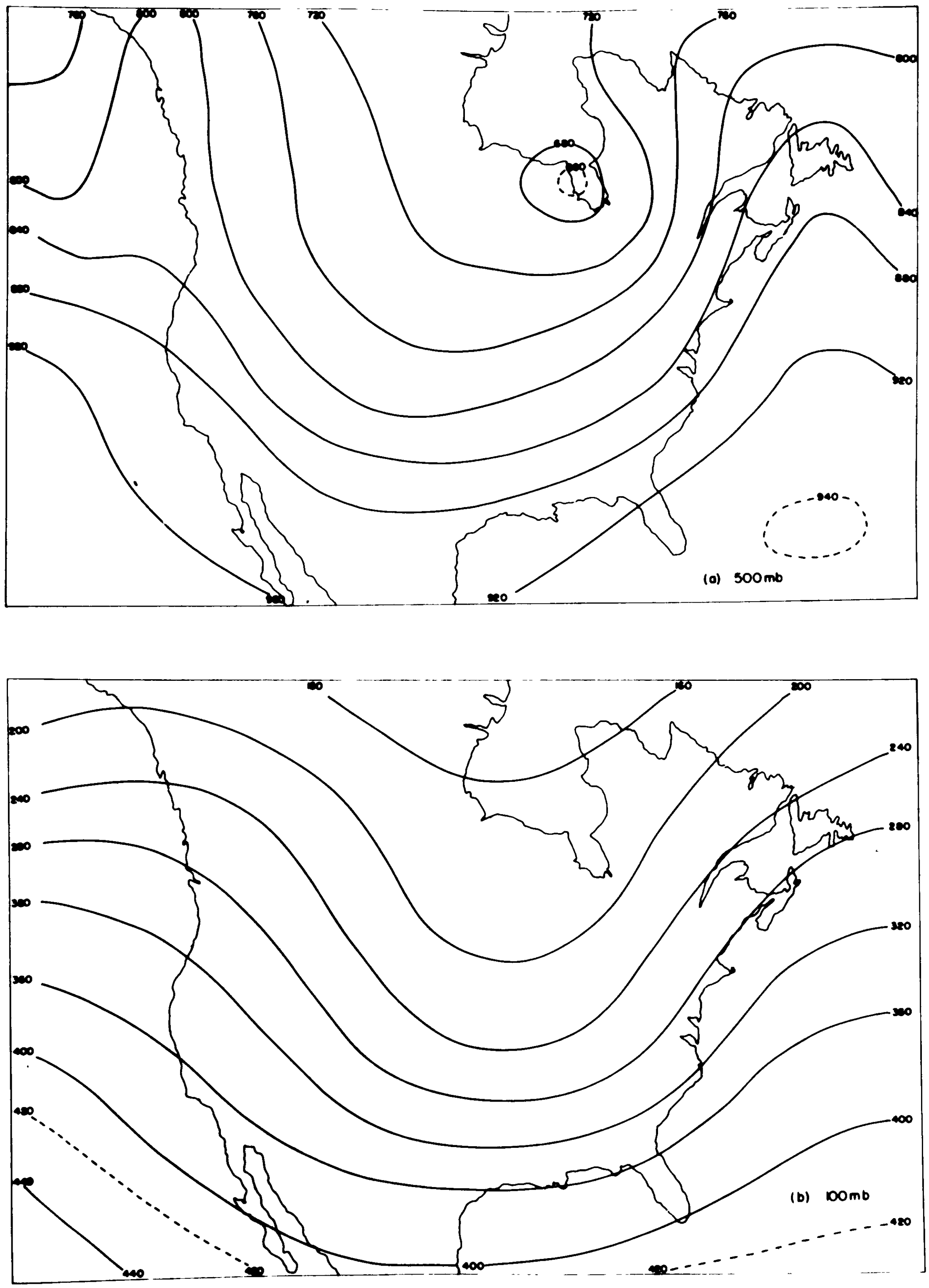

<u>Figure 10</u>. 24-hour barotropic forecasts for 1200 GCT 20 November.

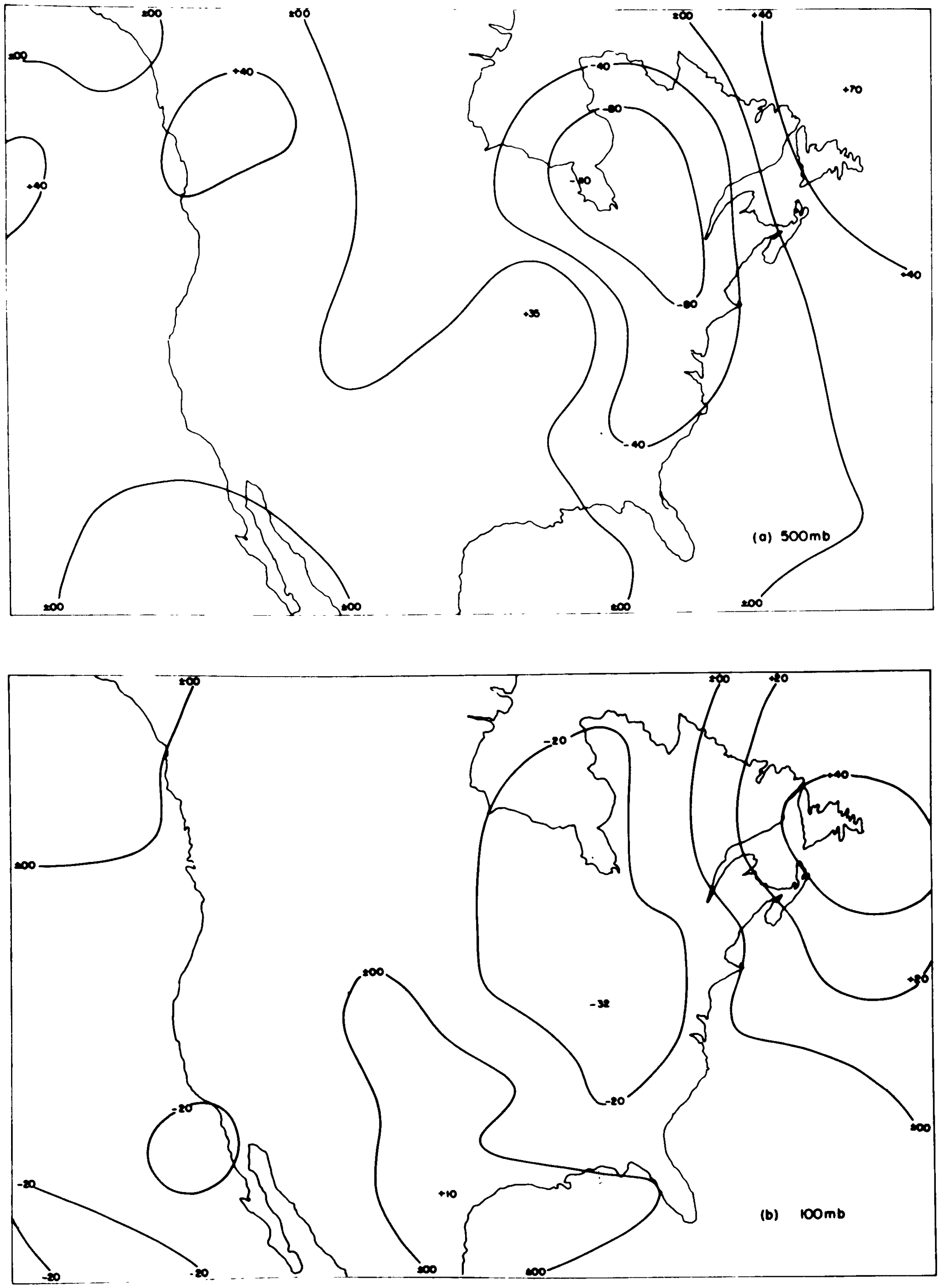

Figure 11. **Observed 24-hour height changes, from 1200 GCT 19 November to 1200 GCT 20 November.**

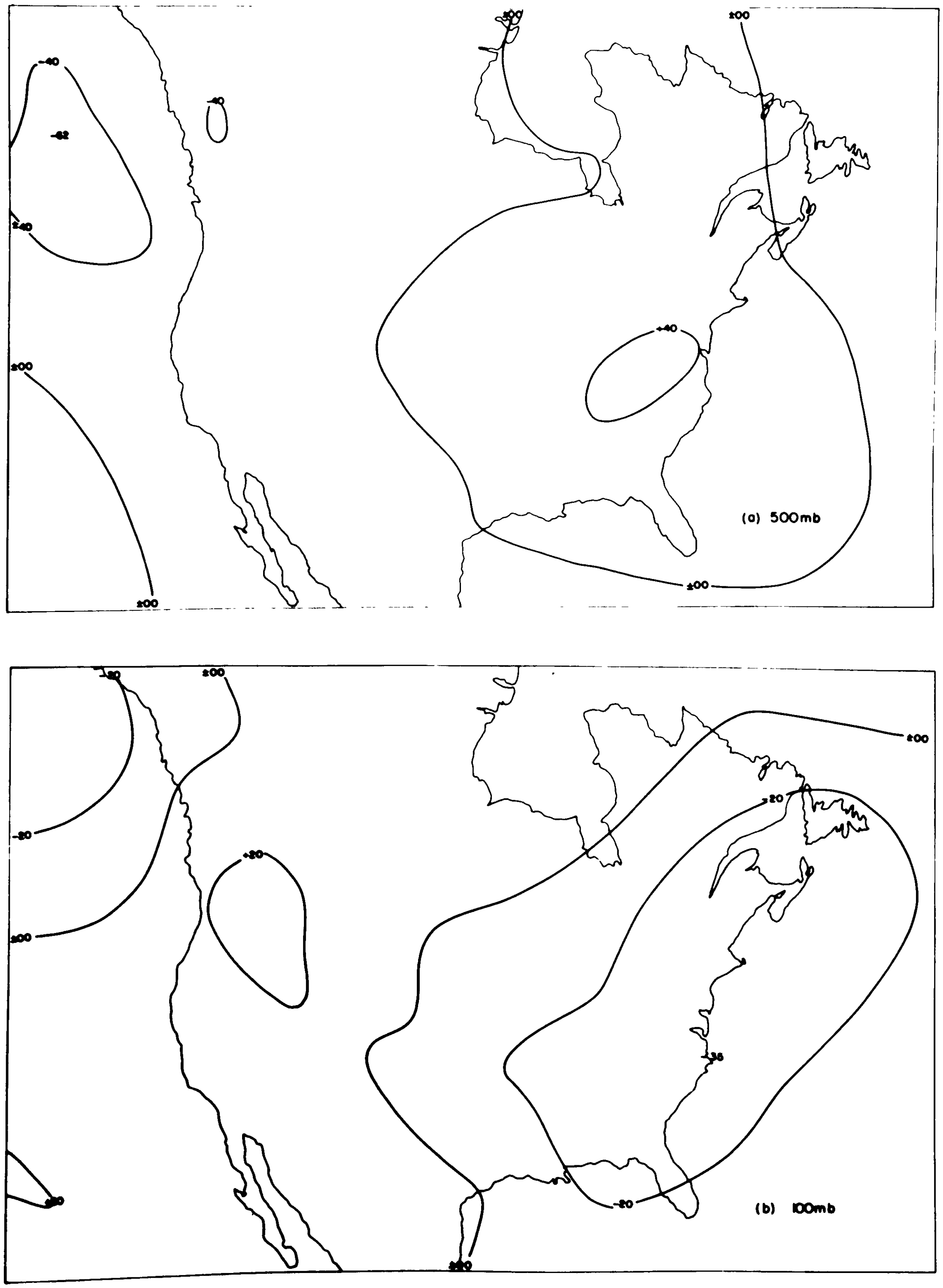

Figure 12. 24-hour-forecast errors, 1200 GCT 20 November.

large and unrealistic errors in prediction would be evident within two or three grid-points of each boundary. The major trough over central North America, except for its southern extremity, is well within the remaining "non-boundary" region, and the prediction of its development was not expected to be affected noticeably by the boundary constraints.

It has been mentioned above (Section II., Part B.) that the lower equivalent-barotropic level over the area of concern is 400 mb, while the predictions are made for 500 mb. The u and A profiles presented in Table A.1 indicate that the values of u, and hence of A, are greater at the 400-mb level than at the 500-mb. From this fact one would expect a portion of the forecast error at 500 mb to be due to an underestimate of the eastward displacement of the trough.

According to Sanders, Wagner, and Carlson (1960) the first 24 hours of the case were a period of rapid development throughout the troposphere over central North America in association with the deepening of an intense sea-level cyclone. The mid-tropospheric height changes of the second 24-hour period, on the other hand, were essentially barotropic in character. It was then concluded that in broad terms the first 24-hour 500-mb forecast would be rather poor, with predicted heights much too high over a large area; the 48-hour, as bad or worse; and the final 24-hour prognosis, the most promising of the entire series.

On the basis of Charney's (1949) and Hinkelmann's (1953) conclusions regarding the propagation of disturbances in the vertical and the vertical extent of influence regions significant for dynamical prediction, it was expected that the 100-mb flow would be affected slightly or not at all by the intense baroclinic development occurring in the troposphere. No other possible sources of forecast error at 100 mb were suggested prior to the actual preparation of the prognoses.

The maps presented in Part A. of this section corroborate the foregoing assertions to a high degree. On the first two 500-mb prognostic charts (Figs. 2(a) and 6(a)) and the corresponding error maps (Figs. 5(a) and 9(a)) the effects of prediction of insufficient trough displacement and of failure to predict the intense development are readily apparent. The lagging of the trough is still in evidence on the second 24-hour forecast map (Fig. 10(a)) and its accompanying error field (Fig. 12(a)), but the actual deepening of the low center was forecast nearly perfectly.

The height changes at 100 mb, as proposed above, reflect essentially no influence of the lower-level baroclinic development. Rather, the errors obtained in barotropic prediction of the 100-mb flow, as one may readily deduce from the prognostic (Figs. 2(b), 6(b), and 10(b)) and error (Figs. 5(b), 9(b), and 12(b)) maps, are attributable primarily to forecasts of excessive eastward displacement of the trough. The existence of a field of large-scale divergence, positive ahead of the trough and negative (convergence) behind it, was suggested as a possible explanation of this phenomenon. The author was fortunate to have access to computations made with a ten-level numerical model on the same situation, for the study by Sanders, Wagner, and Carlson (1960) cited previously. One of the products of the machine program is a complete set of grid-point vertical velocities (ω) for each of the ten levels, 100 through 1000 mb, in units of 10^{-4} mbsec^{-1}. With the assumption of the boundary condition $\omega_{p=0} = 0$, the finite-difference approximation to the equation of continuity (Eq. (2)) may be written

$$(\nabla \cdot \mathbb{V})_{p=100} = \left(-\frac{\partial \omega}{\partial p}\right)_{p=100} \approx -\frac{1}{2}\omega_{p=200} \times 10^{-2}\, mb^{-1}, \qquad (8)$$

providing a rough estimate of 100-mb divergence. It is only a crude approximation because the vertical motions above 200 mb, while small in magnitude, are highly variable. However, the approximation was considered adequate for the ensuing discussion. Patterns of "divergence" so determined are shown in Fig. 13, for the two times for which the ten-level-model results were available.

Computations were made to assess the magnitudes of the contributions of gradient of vorticity advection and gradient

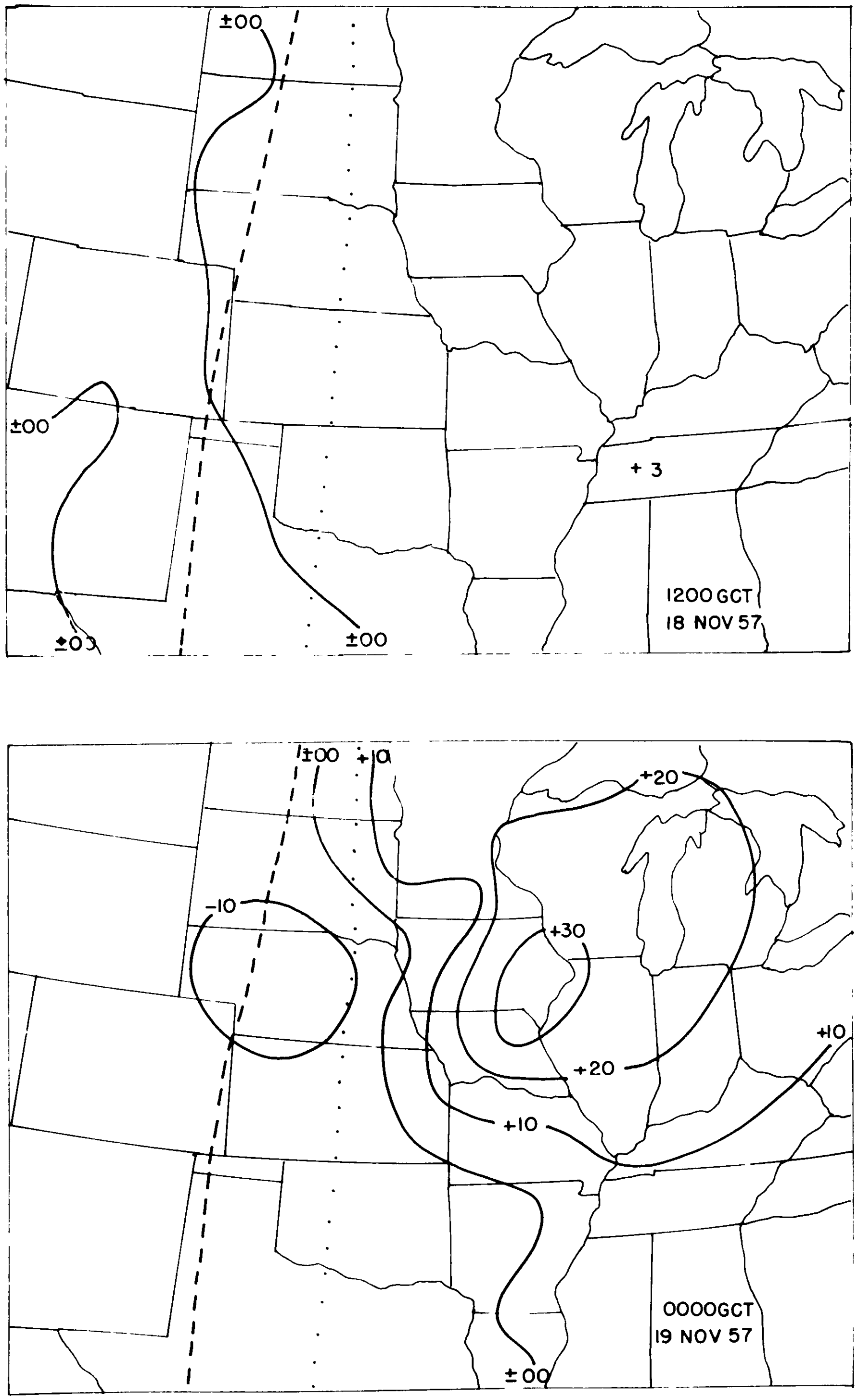

Figure 13. 100-mb "divergence" patterns (unit $10^{-6}sec^{-1}$) determined from ten-level-model vertical velocities (dashed line - trough line on the 18th; dotted line - trough line on the 19th).

of divergence to abetting and/or retarding the eastward movement of the vorticity pattern associated with the trough. The kinematical equation for the speed of the axis of the vorticity pattern, by analogy to Petterssen's (1956) formula for the speed of a pressure-trough axis, is

$$C = -\frac{\frac{\partial}{\partial x}\left(\frac{\partial \zeta}{\partial t}\right)}{\frac{\partial^2}{\partial x^2}(f+\zeta)}, \tag{9}$$

where the x-axis is oriented normal to the vorticity-pattern axis, henceforth denoted "trough line" for convenience. Substitution for $\frac{\partial \zeta}{\partial t}$ from the vorticity equation (Eq. (3)) gives the formula

$$C = -\frac{\frac{\partial}{\partial x}\left[-\mathbb{V}\cdot\nabla(f+\zeta)\right] + \frac{\partial}{\partial x}\left[f_0 \frac{\partial \omega}{\partial p}\right]}{\frac{\partial^2}{\partial x^2}(f+\zeta)}. \tag{10}$$

The derivatives in Eq. (10) were approximated by finite differences and evaluated numerically with the grid-point values of 100-mb height and absolute vorticity for 1200 GCT 18 November provided by the barotropic computer program, and those of $\frac{\partial \omega}{\partial p}$ determined from the ten-level model vertical velocities. For the sake of brevity the first term in the numerator of the right-hand side of Eq. (10) will hereafter be referred to as "V," while the second term will be designated "D."

During the first 24 hours of the case the actual speed of the trough line was 8.8 knots, while the barotropically predicted speed was 17.6 knots. If this difference between predicted and observed speeds were indeed due to the neglect of divergence, then at a given point on the trough line the value of V should be exactly twice that of D.

Values of V, D, and C computed for three points along the trough line (see Table 1) indicate that neither of the assumed "divergence" patterns provides the required effect.

Table 1. CONTRIBUTIONS TO TROUGH-LINE SPEED

$V(nm^{-1}sec^{-2})$	$D_1(nm^{-1}sec^{-2})$	D_2	C_1(kt)	C_2
1.69×10^{-12}	0.87×10^{-12}	-1.06×10^{-12}	17.2	57.5
4.14×10^{-12}	0.73×10^{-12}	-0.38×10^{-12}	20.1	26.7
5.91×10^{-12}	0.19×10^{-12}	1.22×10^{-12}	34.6	28.6

Subscript 1: divergence pattern of 1200 GCT 18 Nov.
Subscript 2: divergence pattern of 0000 GCT 19 Nov.

In addition, the values of V computed from the vorticity print-out (Fig. 14(a)) are all too large compared to the denominator of the right-hand side of Eq. (10) as determined from the same source. Believing the latter discrepancy to be due mainly to small-scale irregularities in the machine-computed vorticities, the author constructed a smooth vorticity pattern (Fig. 14(b)), retaining the essential characteristics of the original. The values of V determined from the

(a)

121	106	148	143	131
121	114	129	133	106
100	113	146	142	082
098	097	152	104	099
082	126	126	119	096

(b)

126	139	148	139	126
120	136	138	136	120
110	129	146	129	110
096	115	150	115	096
092	099	128	099	092

Figure 14. Machine-computed (a) and subjectively smoothed (b) absolute vorticity patterns (unit $10^{-6}sec^{-1}$) associated with trough, for 1200 GCT 18 November 1957.

smoothed vorticity field, and those of D necessary to give the desired speed influence, are presented in Table 2. The relationship between the magnitudes of V and D is very nearly that suggested above.

Table 2. CONTRIBUTIONS TO TROUGH-LINE SPEED AS COMPUTED FROM SMOOTHED VORTICITY

V	D	C
0.99×10^{-12}	0.50×10^{-12}	8.8
2.13×10^{-12}	1.15×10^{-12}	8.8
3.73×10^{-12}	2.26×10^{-12}	8.8

The values of D thus obtained suggest the hypothetical field of divergence shown in Fig. 15. The zero-line is intended to be coincident with the trough line.

-1.06	0	1.06
-2.15	0	2.15
-4.80	0	4.80

Figure 15. Divergence (unit $10^{-6} sec^{-1}$) required to produce derived D-values.

If the true field of divergence is closely approximated by the artificial one derived in the foregoing presentation, then it would serve to retard the motion of the trough very nearly to the extent observed. The neglect of that divergence, implicit in barotropic prediction, would therefore result in a forecast of excessive trough speed.

A measure of the relative goodness of the 500-mb and 100-mb forecasts was obtained by calculating for each level the ratio of root-mean-square forecast height error to root-mean-square observed height change in each forecast period, over a region containing the trough under consideration throughout this discussion. For the 24-hour, 48-hour, and second 24-hour periods, respectively, the ratios are 0.92, 1.24, and 1.23 at 100 mb; and 0.76, 0.79, and 0.51 at 500 mb. Visual comparison of the prognostic and error-field maps (see Figs. 1 - 12) suggests that the 100-mb forecasts are as good as, if not better than, those for the 500-mb level; however, when the magnitudes of the actual height changes are taken into consideration, the 500-mb prognoses reflect a higher degree of forecast skill.

Errors in prediction of features other than the trough discussed at length were considered to contain large contributions due to the boundary conditions, hence of little theoretical interest, and have therefore not been analyzed.

C. Application to Wind Forecasting

Fifteen stations were selected in North America, on the bases of (1) availability of 100-mb wind data on all three days of the case and (2) reasonably great distance from the boundaries of the map. Geostrophic winds were computed for each station from each of the 100-mb prognostic charts and verified against reported observed winds.(see Table 3). Root-mean-square vector errors are 15.2, 22.5, and 15.8 knots for the 24-, 48-, and second 24-hour forecasts respectively; the root-mean-square vector errors in persistence forecasts for the same periods are 19.8, 26.7, and 20.8 knots. In his study of upper-level wind-forecast errors in middle latitudes, Ellsaesser (1957) concluded that at 100 mb persistence gives the best forecast for periods up to 36 and on occasion up to 48 hours, with root-mean-square vector errors of 19.3 knots at 24 hours and 22.8 knots at 48 hours, values comparable to the persistence errors obtained in this study.

While the 100-mb barotropic forecasts are not highly skillful forecasts of the height field (see Section IV., Part B.), the results presented in this section indicate that they provide a wind-forecasting aid that offers substantial improvement over persistence, even at 48 hours. However, because of the small size of the data sample--only 45 forecasts in only one synoptic situation--the author hesitates to draw any final conclusions regarding the general

Table 3. 100-mb WIND FORECAST RESULTS

Station	V^O_{18}	V^F_{19}	V^O_{19}	E^F	E^P
206	2742	2473	2576	14	40
226	2464	2470	2566	13	12
290	3244	3248	3038	18	16
304	2644	2461	2448	13	17
456	2444	3045	2732	24	24
469	3128	3040	3142	8	14
493	3238	3250	2952	26	27
532	2724	2332	2440	10	23
553	2538	2930	2832	6	19
637	2550	2136	2346	18	18
747	2630	2016	2626	18	10
775	3136	3132	3034	7	7
785	2940	3240	3142	8	14
793	2952	3046	3164	20	23
879	3032	2930	3030	5	2

E^F_{rms} = 15.2 kt

E^P_{rms} = 19.8 kt

V(ddff): dd is direction in decadegrees, ff speed in kt.

Superscripts: O is observed, F forecast, P persistence.

Subscripts: day of November 1957.

Table 3. (contd.)

Station	$W_{20}^F(48)$	W_{20}^O	E^F	E^P	$W_{20}^F(24)$	E^F	E^P
206	2672	2664	8	24	2572	15	17
226	2670	27102	35	56	2676	30	46
290	2840	2846	6	31	3046	16	16
304	2560	2470	16	33	2468	2	22
456	3145	2862	32	40	2954	13	32
469	3152	2932	24	12	3155	27	16
493	2735	2954	24	28	2938	15	2
532	2838	2544	22	23	2745	16	8
553	3238	2844	29	22	2942	8	12
637	2625	2444	22	10	2342	8	8
747	3125	2824	13	11	2817	7	9
775	3145	3236	12	6	3242	6	13
785	3045	3120	26	22	3038	18	22
793	2840	3046	16	10	3136	12	20
879	3028	3252	28	24	3235	17	26

48 hours: $E_{rms}^F = 22.5$ kt

$E_{rms}^P = 26.7$ kt

24 hours: $E_{rms}^F = 15.8$ kt

$E_{rms}^P = 20.8$ kt

usefulness of equivalent-barotropic prediction of 100-mb flow as a wind-forecasting tool for that level. A much larger sample of data must be obtained in order to test the results of such a study for statistical significance. Nevertheless, the data presented here are encouraging.

V. SUMMARY AND CONCLUSIONS

The equivalent-barotropic prognostic equation (Eq. (7)), when solved by high-speed digital computation, provides forecasts of 100-mb flow with nearly the same degree of skill during periods both developmental (baroclinic) and non-developmental (barotropic) in the troposphere, while the 500-mb barotropic-forecast skill is considerably better for the non-developmental phase of the situation. In all of the forecast periods, however, greater skill obtains at 500 mb than at 100 mb. The primary source of 100-mb forecast error is the overprediction of trough speed, which is apparently due to the existence of a large-scale pattern of divergence. While the magnitude of this divergence is small, its gradient is sufficiently strong to offset the intense vorticity advection across the trough line and hence retard the movement of the trough. It is true, of course, that divergence is present at 500 mb as well; however, mid-tropospheric vertical motions tend to attain their maximum intensities at or near the 500-mb level, and consequently (see Eq. (2)) the divergence pattern is weak and poorly organized, in contradistinction to the systematic pattern found at 100 mb. Therefore the "divergence effect" discussed at length in Part B. of Section IV. tends to produce the systematic error noted above at 100 mb, but not at 500 mb.

Despite the relative lack of skill of the 100-mb prognoses as compared to those for 500 mb, the former provide a wind-forecasting tool whose use yields substantial improvement over persistence.

Since the inception of routine barotropic 500-mb prediction, the research staff of the Joint Numerical Weather Prediction Unit have added several refinements to the original program. One of these is the hemispheric 1977-point computational grid, which greatly alleviates the problem of "boundary poisoning" inherent in the use of a small rectangular grid such as that employed in the present work. Prediction on a larger grid would permit the study of a larger number of features of synoptic and dynamical interest.

The results of this thesis indicate two other primary areas in which further investigation is desirable. The present equivalent-barotropic computational scheme should be applied to several situations in order to ascertain whether or not the divergence problem is inherent in 100-mb barotropic prediction. If so, it must be concluded that the 100-mb level is not an equivalent-barotropic level in the sense that the 500-mb level very nearly is. That is, at the latter level divergence is not a significant source of error in barotropic forecasting.

Secondly, a much greater effort at 100-mb wind forecasting is required, to determine the statistical significance of the improvement over persistence demonstrated in the small data sample included here. Comparison should also be made of the relative skill of this and other high-altitude wind-forecasting techniques, such as, for example, linear regression based on winds at lower levels.

While limited in scope, the results of the present investigation provide a basis for considerable further study in the realm of high-altitude flow-pattern and wind prediction.

APPENDIX

1. Geostrophic determination of equivalent-barotropic levels between 70W and 125W at 1200 GCT 18 November 1957.

Maps of isobaric height were available for the pressure levels of 1000, 850, 700, 500, 400, 300, 250, 150, and 100 mb. Values were read off at an array of latitude-longitude intersections: 25, 35, 45, 55N; 70, 75, 80, ..., 125W. The values along each latitude were then averaged, and from the zonal-mean heights, mean zonal geostrophic wind components were computed for the latitudes 30, 40, 50N. This procedure was applied to all of the available constant-pressure charts, after which values of u for the levels 900, 800, 600, and 200 mb were determined by linear interpolation.

The pressure-average or "bar" operation was accomplished by means of the approximation

$$\overline{(\ )} = \frac{1}{20}(\ )_{1000\text{ mb}} + \frac{1}{10}\left[(\ )_{900} + (\ )_{800} + \cdots + (\ )_{100}\right]. \quad \text{(A.1)}$$

Values of A, the equivalent-barotropic modeling coefficient, were obtained by use of the relation

$$u = A\,\overline{u}\ . \quad \text{(A.2)}$$

In Table A.1 are presented the u- and A-profiles determined by the above procedure, as well as profiles of A^2 and values of $\overline{u}$ and $\overline{A^2}$ for each latitude.

Table A.1. VERTICAL WIND-SPEED PROFILES, DETERMINED GEOSTROPHICALLY BETWEEN 70W and 125W

	50N			40N		
p(mb)	u(kt)	A	A^2	u	A	A^2
1000	4.4	0.1978	0.0391	- 3.0	-0.1094	0.0120
900	4.6	0.2067	0.0427	3.4	0.1240	0.0154
800	13.8	0.6202	0.3846	10.2	0.3720	0.1384
700	16.6	0.7461	0.5567	15.4	0.5616	0.3154
600	21.1	0.9483	0.8993	21.6	0.7877	0.6205
500	25.6	1.1506	1.3239	27.8	1.0139	1.0280
400	32.6	1.4652	2.1468	41.5	1.5135	2.2907
300	37.4	1.6809	2.8254	54.8	1.9985	3.9940
200	42.3	1.9011	3.6142	58.6	2.1371	4.5672
100	26.3	1.1820	1.3971	42.4	1.5463	2.3910
$\overline{(\;)}$	22.25	1.0	1.3210	27.42	1.0	1.5367

Table A.1. (contd.)

30N

p(mb)	u(kt)	A	A^2
1000	- 3.3	-0.1127	0.0127
900	4.2	0.1434	0.0206
800	12.4	0.4235	0.1794
700	16.1	0.5499	0.3024
600	25.6	0.8743	0.7644
500	35.0	1.1954	1.4290
400	45.6	1.5574	2.4255
300	52.4	1.7896	3.2026
200	58.6	2.0014	4.0056
100	44.6	1.5232	2.3201
$\overline{(\ )}$	29.28	1.0	1.4656

2. Determination of equivalent-barotropic levels for the Northern Hemisphere in winter.

The same calculations performed in deriving Table A.1 were used to obtain Table A.2, except that values of u obtained by Buch (1954) were utilized.

Table A.2. VERTICAL WIND-SPEED PROFILES, DETERMINED FROM BUCH'S HEMISPHERIC WIND DATA

	50N			40N		
p(mb)	u(msec^{-1})	A	A^2	u	A	A^2
1000	1.6	0.1660	0.0276	2.0	0.1534	0.0235
900	3.7	0.3838	0.1473	4.7	0.3604	0.1299
800	5.8	0.6017	0.3620	7.4	0.5675	0.3221
700	7.9	0.8195	0.6716	10.1	0.7745	0.5999
600	9.8	1.0166	1.0335	12.9	0.9893	0.9787
500	11.9	1.2344	1.5237	15.7	1.2040	1.4496
400	13.2	1.3693	1.8750	18.1	1.3880	1.9265
300	14.4	1.4938	2.2314	20.5	1.5721	2.4715
200	15.8	1.6390	2.6863	22.5	1.7255	2.9774
100	13.1	1.3589	1.8466	17.5	1.3420	1.8010
$\overline{(\;)}$	9.64	1.0	1.2391	13.04	1.0	1.2668

Table A.2. (contd.)

30N

p(mb)	u($msec^{-1}$)	A	A^2
1000	- 1.3	-0.1204	0.0145
900	1.2	0.1111	0.0123
800	3.7	0.3426	0.1174
700	6.2	0.5741	0.3296
600	9.8	0.9074	0.8234
500	13.4	1.2407	1.5393
400	16.6	1.5370	2.3624
300	19.7	1.8241	3.3273
200	21.0	1.9444	3.7807
100	17.0	1.5741	2.4778
$\overline{(\;)}$	10.80	1.0	1.4777

REFERENCES

Buch, H., 1954: Hemispheric wind conditions during the year 1950. Final Report Part 2, General Circulation Project, AF 19(122)-153, Dept. of Meteor., MIT.

Charney, J.G., 1948: On the scale of atmospheric motions. Geofys. Publ. 17, 2, 17 pp.

_____________, 1949: On a physical basis for numerical prediction of large-scale motions in the atmosphere. J. Meteor. 6, 6, 371-385.

_____________, and Eliassen, A., 1949: A numerical method for predicting the perturbations of the middle-latitude westerlies. Tellus 1, 2, 38-54.

Ellsaesser, Maj. H.W., 1957: An investigation of the errors in upper-level wind forecasts. Air Weather Service Technical Report AWS TR 105-140/2, Air Weather Service (MATS), USAF.

_____________________, 1960: JNWP Operational Models. JNWP Office Note No. 15 (Revised), Joint Numerical Weather Prediction Unit, National Meteorological Center.

REFERENCES (contd.)

Hinkelmann, K., 1953: Zur numerischen Wettervorhersage mittels Relaxationsmethode unter Einbeziehung barokliner Effekte.II. Tellus 5, 4, 499-512.

Petterssen, S., 1956: Weather Analysis and Forecasting, 2d ed., Vol. I., McGraw-Hill, New York, p. 48

Phillips, N.A., 1958: Lecture Notes on Numerical Weather Prediction (unpublished), Dept. of Meteor., MIT.

Sanders, F., Wagner, A.J., and Carlson, T.N., 1960: Specification of cloudiness and precipitation by multilevel dynamical models. Scientific Report No. 1, AF 19(604)-5491, Dept. of Meteor., MIT.